sustainability

MDPI

Article

Adsorption Studies of Arsenic(V) by CuO Nanoparticles Synthesized by *Phyllanthus emblica* Leaf-Extract-Fueled Solution Combustion Synthesis

Sadia Saif [1,*], Syed F. Adil [2,*], Mujeeb Khan [2], Mohammad Rafe Hatshan [2], Merajuddin Khan [2] and Farzana Bashir [3]

[1] Department of Environmental Science, Kinnaird College for Women, Lahore 54000, Pakistan
[2] Department of Chemistry, College of Science, King Saud University, Riyadh 11451, Saudi Arabia; kmujeeb@ksu.edu.sa (M.K.); mhatshan@ksu.edu.sa (M.R.H.); mkhan3@ksu.edu.sa (M.K.)
[3] Centre for Environmental Protection Studies, PCSIR Laboratories Complex, Lahore 54000, Pakistan; beefarzana@gmail.com
* Correspondence: sadia.saifpk@gmail.com (S.S.); sfadil@ksu.edu.sa (S.F.A.); Tel.: +92-332-4543310 (S.S.); +966-11-4670439 (S.F.A.)

Abstract: In the present study, a simple and eco-friendly route for the synthesis of copper oxide nanoparticles (CuO NPs) using leaf extract of *Phyllanthus emblica* as fuel has been demonstrated, as *P. emblica* is a locally available abundant plant. The formation of the as-prepared CuO NPs was confirmed by using various techniques, such as UV–Vis absorption spectroscopy, cold field scanning electron microscopy (CF–SEM), energy dispersive X-ray analysis (EDX), dynamic light scattering (DLS), and X-ray photoelectron (XPS). The hydrodynamic size of the CuO NPs was found to be 80 nm, while the zeta potential of −28.6 mV was obtained. The elemental composition was confirmed by EDX analysis accompanied with elemental mapping, while the crystalline nature was substantiated by the XRD diffractogram. The as-synthesized CuO NPs were studied for their use as an adsorbent material for the removal of As(V) from water. It was confirmed that the CuO NPs effectively removed As(V) via adsorption, and the adsorption efficiency was found to be best at a higher pH. The maximum adsorption capacity of CuO for As(V) was found to be 1.17 mg/g calculated using the Langmuir equation.

Keywords: CuO; nanoparticles; green synthesis; arsenic; adsorption

Citation: Saif, S.; Adil, S.F.; Khan, M.; Hatshan, M.R.; Khan, M.; Bashir, F. Adsorption Studies of Arsenic(V) by CuO Nanoparticles Synthesized by *Phyllanthus emblica* Leaf-Extract-Fueled Solution Combustion Synthesis. *Sustainability* **2021**, *13*, 2017. https://doi.org/10.3390/su13042017

Academic Editor: Van Khanh Nguyen

Received: 29 November 2020
Accepted: 9 February 2021
Published: 13 February 2021

1. Introduction

Arsenic, a frightful element in ground water, is an element that occurs naturally in trace amounts commonly found in the earth's crust. Typically, it seeps into the groundwater due to various anthropogenic activities, such as coal ash disposal, mining, wood preservation, pesticide application, along with the natural weathering processes. In the aqueous solutions, it commonly exists in two oxidation states, such as As(III) and As(V) [1]; commonly, the toxicity of these elements is highly prevalent in developing countries, which are struggling to overcome this menace. Indeed, arsenic toxicity has turned into a principal concern, as it is significantly accelerating the contamination of important sources of human life, including water, air, and soil. Moreover, the concern levels are upended due to its capability to readily convert its oxidation state, thus displaying diverse chemical behavior; this leads to the formation of a large number of organic and inorganic compounds in the environment.

Among various sources, the main pathway of arsenic exposure around the globe has been reported to be drinking water [2]. Moreover, higher arsenic levels in groundwater pose a serious threat to the public health and other lives on earth, as reported in many countries around the world. [3] It is responsible for the development of various ailments, such as different types of cancers and many other diseases caused due to the contamination

to which humans are regularly exposed by food, water, air, and soil or by long-term intake of small doses of inorganic arsenic compounds, which seriously affects the biological functions of various cells and tissues [4,5].

The most frequently used methods for the elimination of metal ions from industrial effluents include solvent extraction, membrane filtration, reverse osmosis, ion exchange, and adsorption; however, in order to get rid of the arsenic contamination, in addition to the methods commonly employed, nanofiltration, foam flotation, and biological sequestration are also employed [6–10]. However, adsorption using various nanomaterials is one of the advantageous methods among all the above mentioned techniques for the exclusion of heavy metals from water due to its operational simplicity, substantial efficiency, and low cost [11].

Nanomaterials such as metal nanoparticles, metal nanowires, carbon nanotube, etc., display unique electronic, magnetic, catalytic, optical, and medicinal properties as compared with the traditional and bulk materials due to their quantum size effect, large surface to volume ratio, large surface energy, and spatial confinement [12,13]. Particularly, metal oxide nanoparticles (NMOs), including manganese oxides, ferric oxides, aluminum oxides, magnesium oxides, titanium oxides, and cerium oxides, have gained immense popularity and were successfully used for the removal of heavy metals from aqueous systems [14,15]. Among the various metal oxides, copper oxide (CuO) and CuO-based nanomaterials, important materials that are largely employed in energy, medical applications, have gained significant attention for the removal of heavy metals from polluted water for environmental remediation due to their high efficiency and low cost. Besides, the large surface area and abundance of active sites on the surface of CuO makes it a reliable adsorbent material for heavy metals, particularly As(V). This is clearly reflected in various earlier studies. For instance, Pillewan reported that more than 95% of As(III) and As(V) was successfully removed by copper oxide fused mesoporous alumina-based material [16]. In another study, Zhang et al. applied Fe-Cu binary oxide, a low-cost material prepared using a facile method as an effective adsorbent for the exclusion of both As(V) and As(III) from water and has displayed excellent performance [17]. Moreover, CuO-based materials are also regard as proficient adsorbents for water purification due to their low toxicity and negligible solubility in the water. For example, in a recent study, Hassan et al. used CuO NPs as an adsorbent to separate Cd (II) and Ni (II) ions from its aqueous solutions.

So far, different physical and chemical approaches have been reported to fabricate copper oxides nanoparticles with different size, shape, and morphology. These include precipitation pyrolysis, sol-gel technique, electrochemical, sonochemical, solid-state reaction, hydrothermal process, thermal synthesis, microemulsion system, quick-precipitation, thermal decomposition of precursors, microwave irradiations, etc.

However, the CuO NPs prepared from chemical methods usually possess enhanced toxicity due to the adsorption of hazardous chemicals on the surface of NPs during the synthesis. Due to this, the biocompatibility of the resulting material is seriously affected, which ultimately limits the medical applications of CuO-based materials. Therefore, researchers are constantly making enormous attempts to synthesize nanoparticles by green approach. Particularly, nanoparticle synthesis using green methods has gained significant attention in the recent years.

Green synthesis of metallic and metal oxide NPs using environmentally friendly materials such as plant extracts has gathered much more attention due to the mounting necessity to develop such a technology [18]. Recently, eco-friendly preparation of various metal oxide nanoparticles using plant-based materials has also attracted significant attention. These approaches are environmentally benign and can be easily performed using simple reaction system under mild reaction conditions. Particularly, the use of nontoxic reagents and solvents, such as water, easy scale up, and cost effectiveness has significantly enhanced the biocompatibility of these approaches in biomedical and pharmaceutical applications. Moreover, nanoparticles prepared by the use of plant extract enhanced biocompatibility and stability, in comparison with those produced by chemical methods [19]. Therefore,

plant extracts have been established as excellent materials for the easy, large-scale, and eco-friendly synthesis of well-dispersed metal and metal oxide nanoparticles of controlled shapes and sizes [20].

In this regard, many plants have been explored for the synthesis of copper oxide nanoparticles. For instance, tea leaf and coffee powder extracts were applied under microwave irradiations for the synthesis of CuO NPs [21,22]. Moreover, the plant-based synthesized CuO nanoparticles have been used efficiently in various biological and non-biological activities including cytotoxicity [23], antibacterial [24,25], catalytic activity [26,27], photocatalytic treatment of dye [28], degradation of dyes [29], etc. However, as the toxicity of CuO NPs is of concern, we studied the toxicity of the CuO NPs fabricated by utilizing *Pterospermum acerifolium* leaf extract. It was found that *P. acerifolium*-mediated copper oxide NPs were more stable than the engineered CuO NPs and showed less toxicity as compared to engineered CuO NPs when tested on *Daphnia*. The toxic values EC_{50} (effective concentration 50) were observed for engineered CuO NPs, i.e., 0.102 ± 0.019 mg/L, while 0.69 ± 0.226 mg/L for *P. acerifolium*-synthesized CuO NPs [20]. Hence, it was concluded that the green-synthesized CuO NPs are less toxic than the chemically synthesized CuO NPs.

Phyllanthus emblica has been utilized for many purposes, and all its parts including fruits, leaf, and bark have been utilized for medicinal applications. It is widely cultivated in different regions of Asia and native to Pakistan, while it is the least researched plants [30,31]. Hence, in continuation of our research being carried out by our group [32–36], in the present study, we have demonstrated the synthesis of CuO NPs using a solution combustion method using the leaf extract of *P. emblica* as fuel, which is a green alternative to synthetic-organic-compounds-based fuel such as glycine, urea, carboxymethylcellulose, DL-malic acid [37,38]. The synthesized nanoparticles were characterized by different techniques. Furthermore, we also investigated the adsorption capacity of freshly prepared CuO NPs for the removal of arsenic (V).

2. Materials and Methods

P. emblica leaves were sourced from botanical Jinnah Garden Lahore Pakistan, Copper nitrate trihydrate $Cu(NO_3)_2{\cdot}3H_2O$, sodium arsenate dibasic heptahydrate ($Na_2HAsO_4{\cdot}7H_2O$), 69% nitric acid (HNO_3) analytical grade solvents were purchased from Sigma-Aldrich. Arsenic standard solution (1000 µg/mL arsenic in 2% HNO_3) was purchased from High Purity Standards, USA. Milli-Q water was used in all experiments.

2.1. Green Synthesis of CuO NPs

CuO nanoparticles were prepared by ecofriendly green combustion route using *P. emblica* leaves extract as a fuel as described in previous study [20].

Aqueous leaf extract was prepared by extracting 20g powder in 100 ml D.I water and was carefully filtered. An amount of 3.8 g copper $Cu(NO_3)_2{\cdot}3H_2O$ was added in 10 mL of extract and then mixed thoroughly by a magnetic stirrer at 45–50 °C. Dark green solution of salt and extract was placed in a preheated furnace at 400 °C for 5 min. Black-obtained product was stored in an air tight container for further characterization and applicability studies.

2.2. Characterization of CuO NPs

UV-visible absorption spectroscopy was performed by the UV-visible spectrophotometer (UV-1800; Shimadzu, Tokyo, Japan). Cold field emission scanning electron microscopy (equipped with EDX) was employed for determination of morphology, size, and chemical composition of CuO NPs (CFE-SEM, SU8230, Hitachi, Tokyo, Japan). For the determination of zeta potential and hydrodynamic size, a dynamic light scattering (DLS) Nano-ZS instrument (Malvern Instruments Ltd., Malvern, UK) was used. Surface elemental composition was investigated by the X-ray Photoelectron Spectrometer (XPS) System, (Thermo Scientific™ K-Alpha^{+}™X-ray Waltham, MA, USA). Crystalline nature of the synthesized

product was analyzed through X-ray powder diffraction (XRD) (Bruker D8 Advance, Karlsruhe, Germany) patterns using a Cu Kα radiation (λ = 1.54 Å) source in the range of 2θ from 20–80°.

2.3. Adsorption Experiments

Solutions of As(V) of different concentrations were prepared by diluting the stock solution of sodium arsenate with water. Various factors such as initial As(V) concentration, dose of CuO-NPs, pH, time duration of treatment were studied. ICP-OES was used for determination of arsenic concentration in samples.

% *removal efficiency* was calculated by following formula.

$$\%\ Removal\ efficiency = \frac{C_0 - C_i}{C_0} \times 100 \quad (1)$$

Adsorption kinetics and isotherms were investigated in batch adsorption experiments.

For adsorption isotherm, CuO nanoparticles adsorbent was used in batch experiments at different initial concentrations of As(V) (0.5–15 mg/L) with a constant weight of adsorbents (1 g/L). Contact time of 50 min and pH 8 ± 0.3 was used. Equilibrium adsorption capacity (q_e) was calculated from the above given formula.

The amount of metal ions adsorbed at equilibrium (q_e) per unit mass of the adsorbent was calculated by the expression:

$$q_e = \frac{C_0 - C_e}{m} \times V \quad (2)$$

q_e represents adsorption capacity (mg/g).

C_0 and C_e are the initial concentration and final concentrations of arsenic mg/L, respectively.

V is volume of arsenic solution (L).

m is the mass of adsorbent (g).

For CuO adsorbent, the experiments were carried out by placing 1 g/L of adsorbent in different conical flasks containing 200 mL As(V) solution with different initial concentrations of arsenic 1–5 mg/L (pH = 8.0 ± 0.1, at 24 °C). The amount of sorption at time t, q_t (mg/g), was calculated using the following formula:

$$q_t = \frac{C_0 - C_t}{m} \times V \quad (3)$$

Here, q_t is adsorption capacity (mg/g) at time "t". C_t (mg/L) is the concentration of arsenic at any time, C_0 (mg/L) is the initial concentration of arsenic in solution. V is the volume of the solution (L), and m is the mass of adsorbent (g).

3. Results and Discussion

3.1. Characterization of CuO NPs

3.1.1. UV-Vis Spectral Analysis

In order to confirm the formation of CuO nanoparticles, the prepared sample was subjected to UV-vis analysis, and the spectra obtained are given in Figure 1; it reveals that the absorption peak of *P. emblica* leaves extract appears in the region of 300–350 nm, while for its corresponding CuO nanoparticles, the absorption peak was observed at ~400 nm, which confirms the formation of the desired CuO nanoparticles. Typically, the characteristic absorption peak of CuO is observed in the range of 200 to 500 nm depending upon the particle size. The absorption peak of bulk CuO appear at the higher wavelength (red-shifted); however, the peaks' position is blue-shifted (towards a lower wavelength) as the size of the particles decreases [39]. In an earlier study, in which the CuO NPs was prepared from the extract of heart-wood of *P. marsupium*, the UV absorption peak was observed at slightly higher wavelength ~442 nm, and the size of the nanoparticles was found to be in the range of 20 to 50 nm [40]. However, in this study, the absorption peak of CuO appears

at much lower wavelength (blue-shifted) at ~400 nm, from which it can be anticipated that smaller size of CuO NPs are formed.

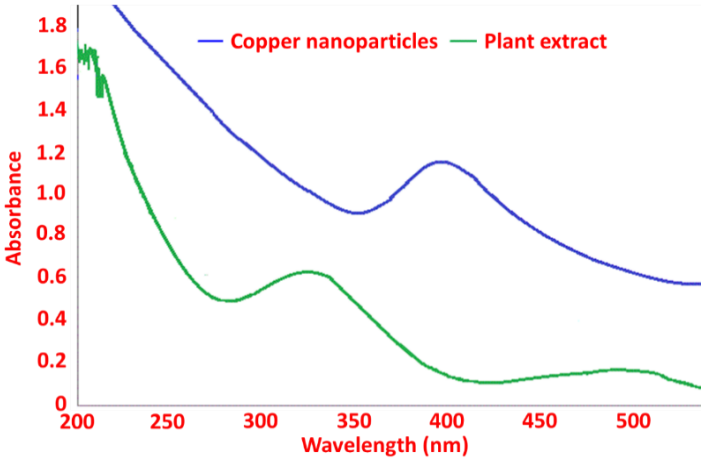

Figure 1. UV-vis spectra of *P. emblica* employed CuO NPs.

3.1.2. SEM and EDX Analysis

The EDX analysis clearly confirms the presence of both copper and oxygen in the sample. While, the SEM analysis was used to identify the surface morphology of as-obtained CuO NPs. From the SEM image, it was observed that the surface of the CuO NPs formed was rugged and was covered with oval shape particles with an average diameter of 80 nm as can be seen in Figure 2. The elemental composition of synthesized CuO nanoparticles was confirmed by EDX analysis and elemental mapping. It confirms the presence of all constituent elements, i.e., copper (Cu) and oxygen (O), confirming the formation of CuO nanoparticles as the prepared product. The other small peaks observed in the EDX spectrum represent the elements Si, K, and Ca can be from the plant extract, which were present in the substrate. The EDX spectra are shown in Figure 3. Hence, we can deduce that the green fuel, i.e., *P. emblica*, may play a profound role in synthesis of pure CuO nanoparticles.

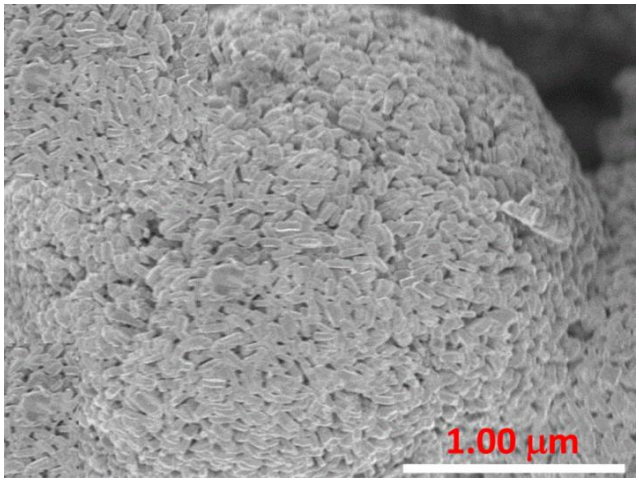

Figure 2. SEM images of *P. emblica*-synthesized CuO NPs.

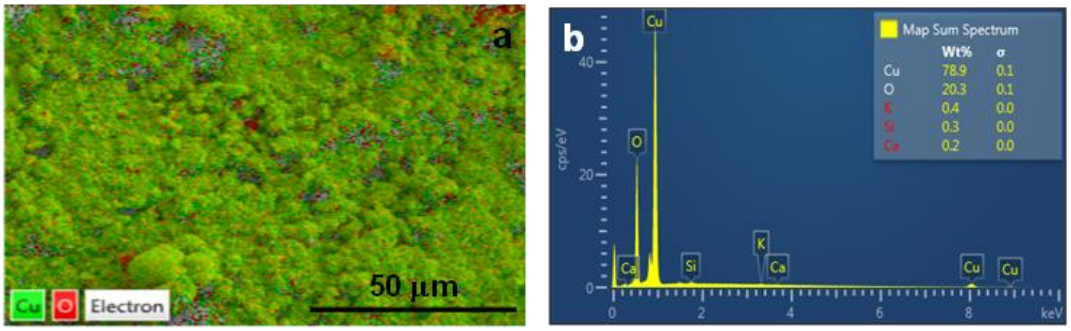

Figure 3. (**a**) Elemental mapping and (**b**) energy dispersive X-ray (EDX) spectrum of the of *P. emblica*-synthesized CuO NPs.

3.1.3. XPS Analysis

In order to confirm the formation of the desired CuO nanoparticles, the as-prepared samples were subjected to various spectral analysis. The XPS survey scan revealed the presence of the Cu and O elements. (Figure 4) The peak binding energy at 934.6 eV and 952.4 eV corresponds to Cu $2p_{3/2}$ and Cu $2p_{1/2}$, respectively. Moreover, binding energy at 531.6 eV corresponds to O 1s of CuO nanoparticles.

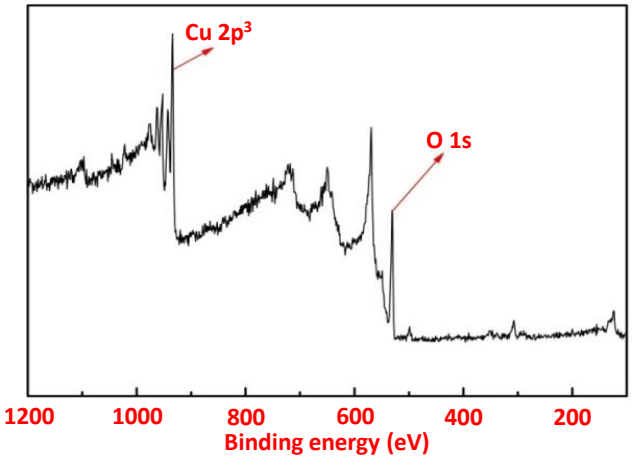

Figure 4. XPS spectra of *P. emblica*-synthesized CuO NPs.

3.1.4. XRD Analysis

The crystalline nature of the as-obtained CuO NPs was identified using the XRD analysis (Figure 5), and the XRD pattern obtained corresponds to the monoclic phase CuO (JCPDS 34-0394), however some several unidentified pattern is also obtained, which can be attributed to the presence of plant extract on the surface of the NPs.

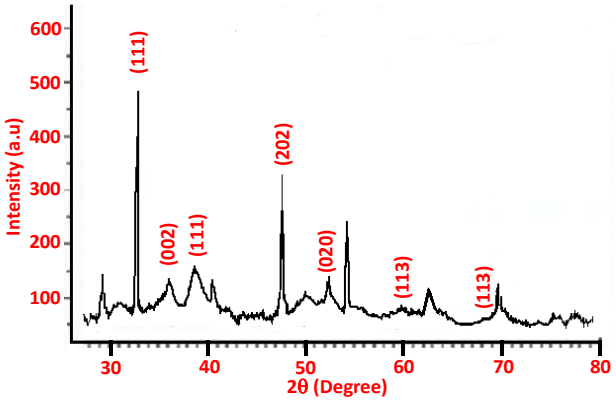

Figure 5. XRD pattern of *P. emblica*-synthesized CuO NPs.

3.1.5. Size/Size Distribution and Zeta Potential Analysis

Hydrodynamic sized for *P. emblica*-synthesized CuO nanoparticles were found to be 92.3 nm, and maximum distribution was at 88.92 nm (Figure 6). This value is much higher than the anticipated average size from the UV-vis analysis, which can be attributed to the agglomeration of the CuO NPs formed, indicating the lower stability of the NPs formed in the absence of capping agent. Zeta potential, which gives critical information on the dispersion of NPs, in terms of magnitude of the charge, which indicates the mutual repulsion between the particles [41]; moreover, the zeta potential values within ± 30 range are reported to be more stable in solution [42]. Earlier, it is reported that the average zeta potential of the CuO nanoparticles occurs in the range of −20 to +45 mV depending upon the pH between 2 to 12 [43]. However, in this case, the higher negative value of zeta potential −28.6 mV can be attributed to the presence of phytomolecules on the surface of CuO NPs (Figure 7).

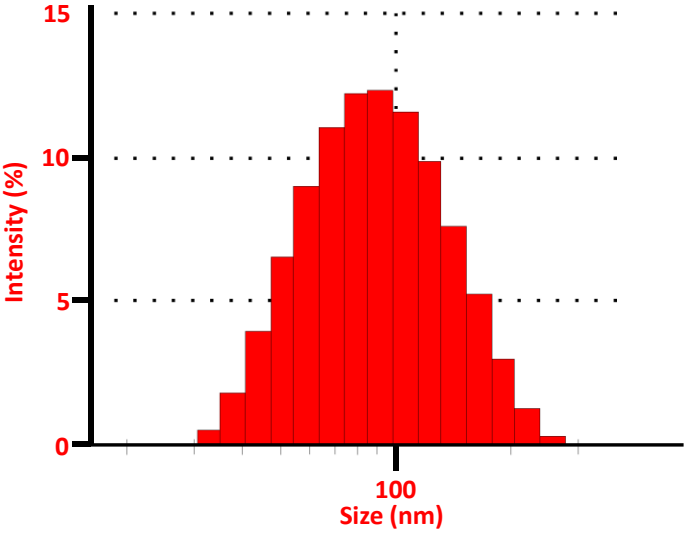

Figure 6. Particle size distribution graph *P. emblica*-synthesized CuO NPs.

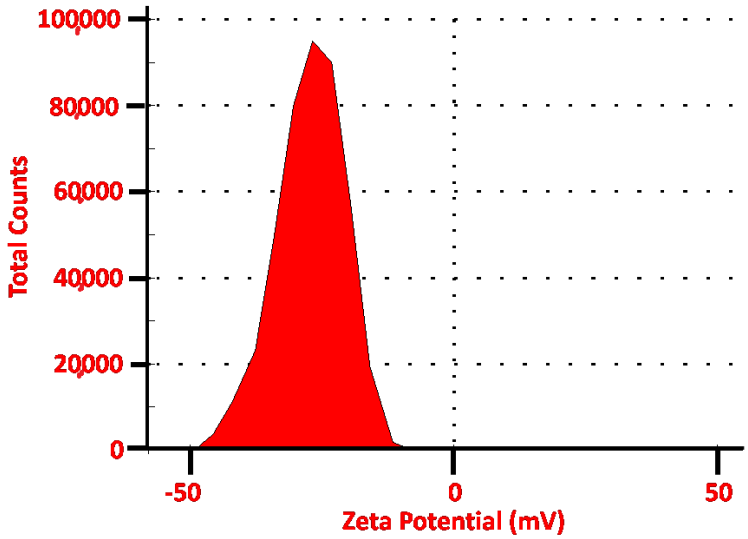

Figure 7. Zeta potential of *P. emblica*-synthesized CuO NPs.

3.2. Arsenic Adsorption Results

3.2.1. Effect of Nanoparticles Dosage and Initial As(V) Concentration

Initially, the effect of adsorbent dosages was determined for the removal of arsenic (V) from water. In this study, a varying amount of *P. emblica*-synthesized CuO NPs, i.e.,

0.1–2.5 g/L, were dispersed in solutions of initial arsenic concentration of 1–15 mg/L, at pH 7 ± 0.4, and the percentage reduction in the As(V) concentration was recoded, and the results obtained are illustrated in Figure 8. It was revealed that the adsorption of arsenic increased from 46 to 85%, with an increase in adsorbent dose, i.e., CuO NPs, from 0.1 to 2.5 g/L, when the solution contained 1 mg/L of As(V). Whereas, in the solution with As(V) concentration of 15 mg/L, the adsorption of arsenic increased from 44 to 71% with an increasing dosage of CuO adsorbent, i.e., from 0.1 to 2.5 g/L. From this study, it can be confirmed that the maximum adsorption of As(V) is obtained when 2.5 g/L of the CuO NPs are employed and the concentration of As(V) is 1 mg/L.

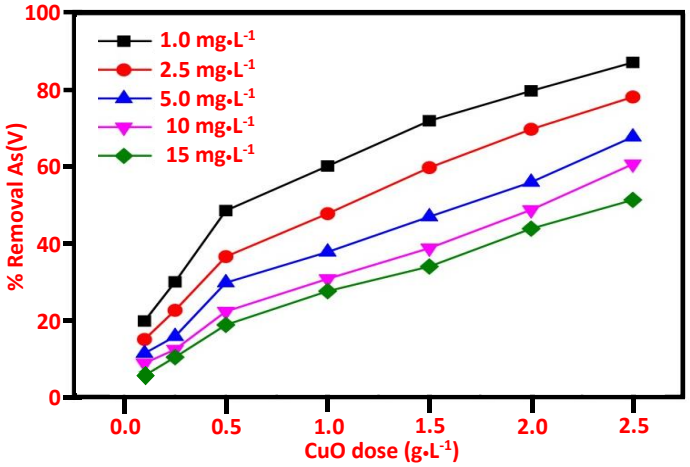

Figure 8. Effect of *P. emblica*-synthesized CuO nanoparticles doses on removal of arsenic at different concentrations of As(V).

3.2.2. Effect of pH on As(V) Removal

It is well reported that the adsorption capacity of an adsorbent varies by changes in the pH. Hence, a study was carried out to ascertain the effect of pH on the removal of As(V) by the CuO NPs, by changing pH from 2–12, and the results obtained are illustrated in Figure 9. From the results obtained, it was found that arsenate adsorption of CuO nanoparticles was 98.9% at pH 12, while the adsorption was lower with lower pH such as 81% at pH 10 and ~66% at pH 8, when the initial As(V) concentration was 1 mg/L (Figure 9). Results showed that the arsenic adsorption capacity of the CuO NPs is influenced by varying the pH, and the best adsorption capacity of CuO NPs is obtained at pH 12, and the least adsorption of ~20% As(V) is obtained at pH 3. The high adsorption at pH 12 can be attributed to the zeta potential, which shifts towards the negative values in the range −12.6 ± 0.4 and −15.7 ± 1.6 mV, indicating the surge in generation of negative charge on the surface of CuO nanoparticles, which more efficiently attract the positive arsenic ions [44]. Another study reported by Goswami et al. reported that by increasing pH, 100% removal of arsenic can be achieved [45]. Hence, it can be concluded that the adsorption efficiency of the CuO NPs is very much dependent on pH, and the best adsorption is obtained under basic conditions.

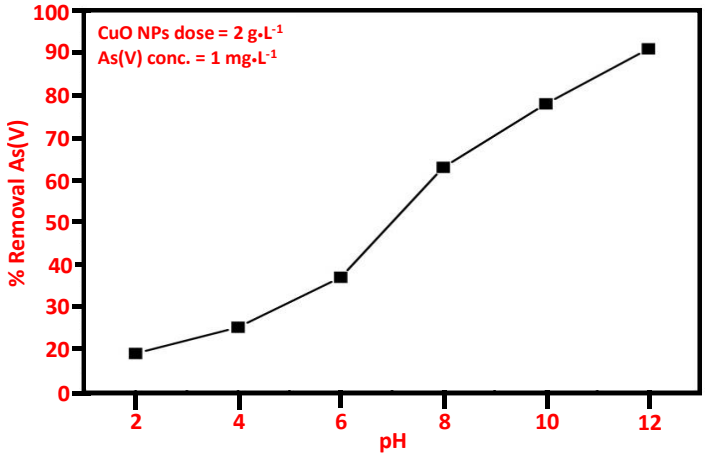

Figure 9. As(V) removal efficiency at different pH levels by *P. emblica*-synthesized CuO NPs.

3.2.3. Effect of Contact Time on As(V) Removal

Contact time plays an important role in the adsorption studies, and hence, the adsorption capacity of As(V) on the surface of CuO nanoparticles with respect to time was also investigated. Different solutions were allowed to react with CuO nanoparticles for a long period of time ranging between 1–14 h with varying initial As(V) concentrations under basic conditions. When the As(V) concentration is 1.0 mg·L^{-1}, it was found that in the first hour of contact, As(V) concentration reduced by 15%, which was followed by a steep rise in the reduction in concentration of As(V), i.e., 75.2%, up to 400 min; however, after this time, the removal of As(V) is very insipid until 800 min of contact time, indicating that the maximum adsorption capacity of the CuO NPs has been achieved in 400 min of contact time. Moreover, when the concentration of As(V) is increased to 2.5, 5, and 10 mg·L^{-1} the reduction in concentration of As(V) was found to be 68, 56.2, and 46%, respectively, after 400 min of contact time. However, it was observed that after 400 min of adsorption, a similar trend of As(V) concentration reduction as seen in 1 mg·L^{-1}, wherein no further decrease in As(V), was observed, indicating that the no further adsorption of As(V) takes place on the surface of the CuO NPs. Figure 10 displays the kinetics of adsorption of As(V) by the CuO NPs.

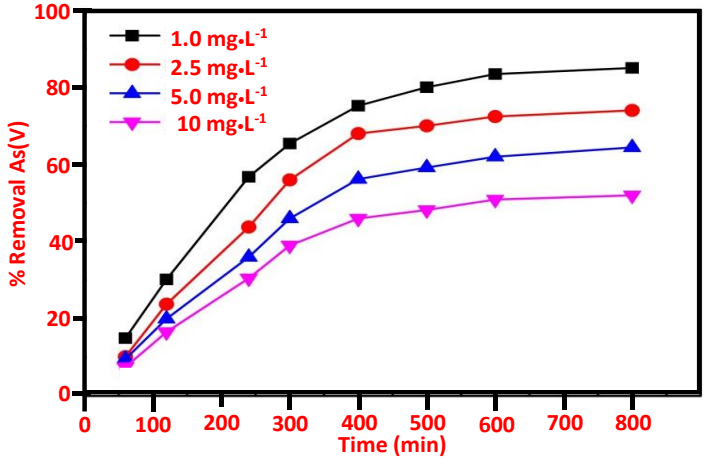

Figure 10. As(V) removal efficiency at different time intervals by *P. emblica*-synthesized CuO NPs.

3.2.4. Adsorption Isotherms

The adsorption capacity of CuO nanoparticles towards As(V) were evaluated using adsorption isotherm with adsorbent dose 1 g/L (Figure 11). Calculated parameters for As(V) adsorption are presented in Table 1. Maximum adsorption capacities were calculated from the Langmuir equation to be 1.17 mg/g for As(V). However, the adsorption data

of As(V) removal by CuO were best fit with Freundlich isotherm ($R^2 > 0.99$). The value of K, the value of 1/n < 1, and the value of n < 10 indicate favorable for Freundlich adsorption isotherm. Moreover, the steep slope (1/n), which is very close to 1, indicates high adsorption capacity at higher equilibrium concentration.

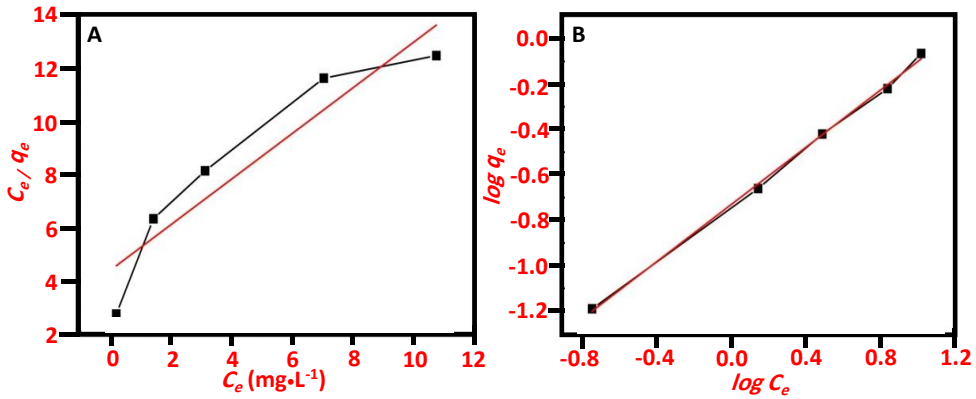

Figure 11. (**A**) Langmuir and (**B**) Freundlich model for *P. emblica*-synthesized CuO NPs.

Table 1. Langmuir and Freundlich isotherms parameters for As(V) adsorption on CuO nanoparticles.

Adsorbents	Langmuir Model			Freundlich Model		
	qm (mg/g)	K_L (L/mg)	R^2	*n*	K_f (mg/g)	R^2
CuO NPs	1.17	0.19	0.876	1.58	0.18	0.999

Initial arsenic concentration 0.5–15 mg/L. contact 60 min. q_m (mg/g) is the maximum adsorption capacity from the Langmuir isotherm. K_L (L/mg) is a Langmuir constant. K_f (mg/g) related to adsorption capacity. *n* is a dimensionless Freundlich constant.

Interestingly, when the obtained adsorption capacities are compared with various other CuO structures prepared by various other approaches, it has been found to possess varying adsorption capacities based on the synthetic methodologies applied for their synthesis. Cao et al. reported the synthesis of copper oxide (CuO) structures using copper acetate as precursor, and the doughnut-like CuO particles were employed for the removal of As(III), and the adsorption capacities were found to be 5.7 mg/g for As(III) [46]. Another example of CuO nanoparticles for the removal of As ions were reported by Martinson et al., which yielded maximum adsorption capacity, was reportedly found to be 26.9 mg/g for As(III) and 22.6 mg/g for As(V) [44]. In another study, spherical CuO nanoparticles of 30 ± 2 nm size were prepared by hydrothermal technique, and a 97.8% percent removal of As(III) was observed, and adsorption capacity K_f 0.6035 mg/g was calculated by the Freundlich isotherm model [47]. As(III) removal was attempted by green-synthesized CuO NPs employing *Tamarindus indica* pulp extract, the adsorption capacity was found to be 1152.5 µg/g, which is very close to the maximum adsorption capacity value, i.e., 1.17 mg/g, obtained from the CuO NPs prepared by the *P. emblica* leaf extract [48]. Hence, it can be concluded that the CuO NPs obtained in the present work are not as efficient as the CuO NPs prepared by the chemical synthesis, indicating that the solution combustion synthesis is the sustainable facile method to produce pure CuO NPs, however the As ions adsorption capacity of the CuO NPs obtained is moderate. Future studies can be designed to carry out surface modification of CuO NPs to enhance its adsorptive capacity.

3.2.5. Adsorption Kinetics

Kinetic pseudo-first-order and pseudo-second-order models were studied for CuO nanoparticles adsorbent. The kinetic models are shown in Figure 12 and used for calculation of As(V) adsorption in relation to time "t".

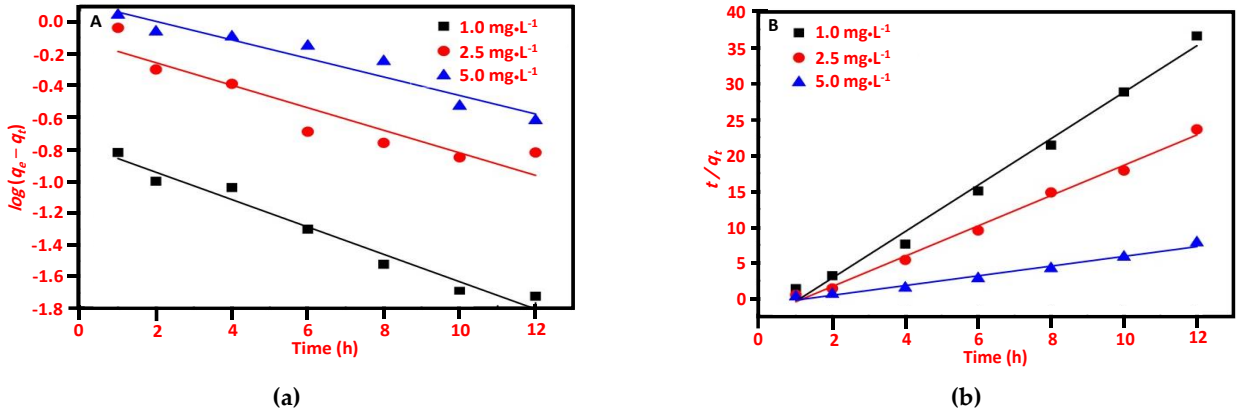

(a) **(b)**

Figure 12. (a) Pseudo-first-order and **(b)** pseudo-second-order sorption kinetics of arsenic by *P. emblica*-synthesized CuO NPs.

The experimental data best fitted with the pseudo-second-order kinetic model and the adsorption process might be chemisorption, which is suitable for sorption at low initial concentrations. Results indicate that rate constants such as K_1 and K_2 of CuO NPs are faster at a lower As(V) concentration (Table 2).

Table 2. Calculated parameters from the pseudo-first model and pseudo-second-order model of adsorption kinetics for CuO nanoparticles.

Adsorbents	Initial As (V) (mg/L)	Pseudo-First-Order Model			Pseudo-Second-Order Model		
		K_1 (min^{-1})	qe ($mg{\cdot}g^{-1}$)	R^2	K_2 ($mg{\cdot}min{\cdot}g^{-1}$)	qe ($mg{\cdot}g^{-1}$)	R^2
CuO NPs	1	0.19	0.16	0.96	1.33	0.30	0.99
	2.5	0.16	0.75	0.87	1.02	0.47	0.99
	5	0.11	1.25	0.91	0.81	1.1	0.99

4. Conclusions

In conclusion, the present study reports the green synthesis of CuO NPs using *P. emblica* leaves extract via solution combustion method was attempted. The formation of green-synthesized CuO NPs was characterized by UV-vis, XRD, and XPS. The microscopic analysis was carried out by SEM, and the images revealed that the CuO NPs formed possessed granular morphology, while the mean diameter of the granules of the CuO NPs formed was found to be 92.3 nm. Moreover, the as-synthesized CuO nanoparticles were employed for the adsorption of As(V), and it was found that the green-synthesized CuO NPs displayed efficient adsorption capacity, which improved up to ~98% at higher pH. The adsorption takes place via a pseudo-second-order mechanism, and the adsorption rate is high when the As(V) are low in concentration. In conclusion, the rapid, simple single-step "green" biosynthesis of CuO NPs is attractive, as it is an ecofriendly protocol, and this protocol can be further employed for the environmental remediation.

Author Contributions: S.S. and F.B. performed the related experiments. S.F.A. and M.R.H. carried out the characterization and arranged funds for the project; S.F.A., M.K. (Mujeeb Khan) and M.K. (Merajuddin Khan) contributed towards writing and editing the manuscript. All authors have contributed, reviewed, and approved the final manuscript.

Funding: This work was supported by Researchers supporting project Number (RSP-2020/222), King Saud University, Riyadh, Saudi Arabia.

Institutional Review Board Statement: Not applicable.

Informed Consent Statement: Not applicable.

Data Availability Statement: Not applicable.

Acknowledgments: The authors would like to acknowledge the Researchers supporting project Number (RSP-2020/222), King Saud University, Riyadh, Saudi Arabia.

Conflicts of Interest: No conflicts of interest.

References

1. Anawar, H.M.; Akai, J.; Komaki, K.; Terao, H.; Yoshioka, T.; Ishizuka, T.; Safiullah, S.; Kato, K. Geochemical occurrence of arsenic in groundwater of Bangladesh: Sources and mobilization processes. *J. Geochem. Explor.* **2003**, *77*, 109–131. [CrossRef]
2. Flora, S.J.S. 1-Arsenic: Chemistry, occurrence, and exposure. In *Handbook of Arsenic Toxicology*; Flora, S.J.S., Ed.; Academic Press: Oxford, UK, 2015; pp. 1–49.
3. Malana, M.A.; Khosa, M.A. Groundwater pollution with special focus on arsenic, Dera Ghazi Khan-Pakistan. *J. Saudi Chem. Soc.* **2011**, *15*, 39–47. [CrossRef]
4. Ghosh, J.; Sil, P.C. 8-Mechanism for arsenic-induced toxic effects. In *Handbook of Arsenic Toxicology*; Flora, S.J.S., Ed.; Academic Press: Oxford, UK, 2015; pp. 203–231.
5. Karim, M.M. Arsenic in groundwater and health problems in Bangladesh. *Water Res.* **2000**, *34*, 304–310. [CrossRef]
6. Mohan, D.; Pittman, C.U., Jr. Arsenic removal from water/wastewater using adsorbents—A critical review. *J. Hazard. Mater.* **2007**, *142*, 1–53. [CrossRef]
7. Han, B.; Runnells, T.; Zimbron, J.; Wickramasinghe, R. Arsenic removal from drinking water by flocculation and microfiltration. *Desalination* **2002**, *145*, 293–298. [CrossRef]
8. Janin, A.; Zaviska, F.; Drogui, P.; Blais, J.-F.; Mercier, G. Selective recovery of metals in leachate from chromated copper arsenate treated wastes using electrochemical technology and chemical precipitation. *Hydrometallurgy* **2009**, *96*, 318–326. [CrossRef]
9. Pous, N.; Casentini, B.; Rossetti, S.; Fazi, S.; Puig, S.; Aulenta, F. Anaerobic arsenite oxidation with an electrode serving as the sole electron acceptor: A novel approach to the bioremediation of arsenic-polluted groundwater. *J. Hazard. Mater.* **2015**, *283*, 617–622. [CrossRef]
10. Mafu, L.D.; Mamba, B.B.; Msagati, T.A. Synthesis and characterization of ion imprinted polymeric adsorbents for the selective recognition and removal of arsenic and selenium in wastewater samples. *J. Saudi Chem. Soc.* **2016**, *20*, 594–605. [CrossRef]
11. Amy, G.L.; Chen, H.-W.; Dinzo, A.; Brandhuber, P. *Adsorbent Treatment Technologies for Arsenic Removal*; Awwa Research Foundation and American Water Works Association: Mumbai, India, 2005.
12. Kelly, K.L.; Coronado, E.; Zhao, L.L.; Schatz, G.C. The Optical Properties of Metal Nanoparticles: The Influence of Size, Shape, and Dielectric Environment. *J. Phys. Chem. B* **2003**, *107*, 668–677. [CrossRef]
13. Cuenya, B.R. Synthesis and catalytic properties of metal nanoparticles: Size, shape, support, composition, and oxidation state effects. *Thin Solid Films* **2010**, *518*, 3127–3150. [CrossRef]
14. Hua, M.; Zhang, S.; Pan, B.; Zhang, W.; Lv, L.; Zhang, Q. Heavy metal removal from water/wastewater by nanosized metal oxides: A review. *J. Hazard. Mater.* **2012**, *211*, 317–331. [CrossRef]
15. Andjelkovic, I.; Stankovic, D.; Jovic, M.; Markovic, M.; Krstic, J.; Manojlovic, D.; Roglic, G. Microwave-hydrothermal synthesis of TiO_2 and zirconium doped TiO_2 adsorbents for removal of As (III) and As (V). *J. Saudi Chem. Soc.* **2015**, *19*, 429–435. [CrossRef]
16. Pillewan, P.; Mukherjee, S.; Roychowdhury, T.; Das, S.; Bansiwal, A.; Rayalu, S. Removal of As(III) and As(V) from water by copper oxide incorporated mesoporous alumina. *J. Hazard Mater.* **2011**, *186*, 367–375. [CrossRef]
17. Zhang, G.; Ren, Z.; Zhang, X.; Chen, J. Nanostructured iron(III)-copper(II) binary oxide: A novel adsorbent for enhanced arsenic removal from aqueous solutions. *Water. Res.* **2013**, *47*, 4022–4031. [CrossRef]
18. Adil, S.F.; Assal, M.E.; Khan, M.; Al-Warthan, A.; Siddiqui, M.R.H.; Liz-Marzán, L.M. Biogenic synthesis of metallic nanoparticles and prospects toward green chemistry. *Dalton Trans.* **2015**, *44*, 9709–9717. [CrossRef]
19. Shaik, M.; Albalawi, G.; Khan, S.; Khan, M.; Adil, S.; Kuniyil, M.; Al-Warthan, A.; Siddiqui, M.; Alkhathlan, H.; Khan, M. "Miswak" based green synthesis of silver nanoparticles: Evaluation and comparison of their microbicidal activities with the chemical synthesis. *Molecules* **2016**, *21*, 1478. [CrossRef]
20. Saif, S.; Tahir, A.; Asim, T.; Chen, Y. Plant mediated green synthesis of CuO nanoparticles: Comparison of toxicity of engineered and plant mediated CuO nanoparticles towards Daphnia magna. *Nanomaterials* **2016**, *6*, 205. [CrossRef]
21. Sutradhar, P.; Saha, M.; Maiti, D. Microwave synthesis of copper oxide nanoparticles using tea leaf and coffee powder extracts and its antibacterial activity. *J. Nanostruct. Chem.* **2014**, *4*, 86. [CrossRef]
22. Kumar, B.; Smita, K.; Cumbal, L.; Debut, A.; Angulo, Y. Biofabrication of copper oxide nanoparticles using Andean blackberry (Rubus glaucus Benth.) fruit and leaf. *J. Saudi Chem. Soc.* **2017**, *21*, S475–S480. [CrossRef]
23. Harne, S.; Sharma, A.; Dhaygude, M.; Joglekar, S.; Kodam, K.; Hudlikar, M. Novel route for rapid biosynthesis of copper nanoparticles using aqueous extract of *Calotropis procera* L. latex and their cytotoxicity on tumor cells. *Colloids Surf. B Biointerfaces* **2012**, *95*, 284–288. [CrossRef]
24. Kiruba Daniel, S.C.G.; Vinothini, G.; Subramanian, N.; Nehru, K.; Sivakumar, M. Biosynthesis of Cu, ZVI, and Ag nanoparticles using *Dodonaea viscosa* extract for antibacterial activity against human pathogens. *J. Nanoparticle Res.* **2012**, *15*, 1–10. [CrossRef]
25. Kumar, P.P.N.V.; Shameem, U.; Kollu, P.; Kalyani, R.L.; Pammi, S.V.N. Green Synthesis of Copper Oxide Nanoparticles Using *Aloe vera* Leaf Extract and Its Antibacterial Activity Against Fish Bacterial Pathogens. *BioNanoScience* **2015**, *5*, 135–139. [CrossRef]

26. Suramwar, N.V.; Thakare, S.R.; Khaty, N.T. One pot synthesis of copper nanoparticles at room temperature and its catalytic activity. *Arab. J. Chem.* **2012**, *9*, S1807–S1812. [CrossRef]
27. Manjari, G.; Saran, S.; Arun, T.; Rao, A.V.B.; Devipriya, S.P. Catalytic and recyclability properties of phytogenic copper oxide nanoparticles derived from *Aglaia elaeagnoidea* flower extract. *J. Saudi Chem. Soc.* **2017**, *21*, 610–618. [CrossRef]
28. Tamuly, C.; Hazarika, M.; Das, J.; Bordoloi, M.; Borah, D.J.; Das, M.R. Bio-derived CuO nanoparticles for the photocatalytic treatment of dyes. *Mater. Lett.* **2014**, *123*, 202–205. [CrossRef]
29. Sankar, R.; Manikandan, P.; Malarvizhi, V.; Fathima, T.; Shivashangari, K.S.; Ravikumar, V. Green synthesis of colloidal copper oxide nanoparticles using Carica papaya and its application in photocatalytic dye degradation. *Spectrochim Acta A Mol. Biomol. Spectrosc.* **2014**, *121*, 746–750. [CrossRef]
30. Abbasi, A.M.; Khan, M.A.; Ahmad, M.; Zafar, M. *Medicinal Plant Biodiversity of Lesser Himalayas-Pakistan*; Springer Science & Business Media: Berlin, Germany, 2011.
31. Jansen, P.; Cardon, D. *Plant Resources of Tropical Africa 3. Dyes and Tannins*; PROTA Foundation Netherland: Wageningen, The Netherlands, 2005.
32. Khan, M.; Khan, M.; Kuniyil, M.; Adil, S.F.; Al-Warthan, A.; Alkhathlan, H.Z.; Tremel, W.; Tahir, M.N.; Siddiqui, M.R.H. Biogenic synthesis of palladium nanoparticles using *Pulicaria glutinosa* extract and their catalytic activity towards the Suzuki coupling reaction. *Dalton Trans.* **2014**, *43*, 9026–9031. [CrossRef]
33. Khan, M.; Khan, S.T.; Khan, M.; Adil, S.F.; Musarrat, J.; Al-Khedhairy, A.A.; Al-Warthan, A.; Siddiqui, M.R.H.; Alkhathlan, H.Z. Antibacterial properties of silver nanoparticles synthesized using Pulicaria glutinosa plant extract as a green bioreductant. *Int. J. Nanomed.* **2014**, *9*, 3551.
34. Khan, M.; Kuniyil, M.; Shaik, M.R.; Khan, M.; Adil, S.F.; Al-Warthan, A.; Alkhathlan, H.Z.; Tremel, W.; Tahir, M.N.; Siddiqui, M.R.H. Plant extract mediated eco-friendly synthesis of Pd@ graphene nanocatalyst: An efficient and reusable catalyst for the Suzuki-Miyaura coupling. *Catalysts* **2017**, *7*, 20. [CrossRef]
35. Saif, S.; Tahir, A.; Asim, T.; Chen, Y.; Adil, S.F. Polymeric Nanocomposites of Iron–Oxide Nanoparticles (IONPs) Synthesized Using Terminalia chebula Leaf Extract for Enhanced Adsorption of Arsenic (V) from Water. *Colloids Interfaces* **2019**, *3*, 17. [CrossRef]
36. Asimuddin, M.; Shaik, M.R.; Fathima, N.; Afreen, M.S.; Adil, S.F.; Siddiqui, R.H.; Jamil, K.; Khan, M. Study of Antibacterial Properties of Ziziphus mauritiana based Green Synthesized Silver Nanoparticles against Various Bacterial Strains. *Sustainability* **2020**, *12*, 1484. [CrossRef]
37. Hossain, M.; Kecsenovity, E.; Varga, A.; Molnár, M.; Janáky, C.; Rajeshwar, K. Solution combustion synthesis of complex oxide semiconductors. *Int. J. Self-Propagating High-Temp. Synth.* **2018**, *27*, 129–140. [CrossRef]
38. Lenka, R.; Mahata, T.; Sinha, P.; Tyagi, A. Combustion synthesis of gadolinia-doped ceria using glycine and urea fuels. *J. Alloys Compd.* **2008**, *466*, 326–329. [CrossRef]
39. Dagher, S.; Haik, Y.; Ayesh, A.I.; Tit, N. Synthesis and optical properties of colloidal CuO nanoparticles. *J. Lumin.* **2014**, *151*, 149–154. [CrossRef]
40. Rajgovind, S.G.; Gupta, D.; Jasuja, N.; Joshi, S. *Pterocarpus marsupium* derived phyto-synthesis of copper oxide nanoparticles and their antimicrobial activities. *J. Microb. Biochem. Technol.* **2015**, *7*, 140–144.
41. Clayton, K.N.; Salameh, J.W.; Wereley, S.T.; Kinzer-Ursem, T.L. Physical characterization of nanoparticle size and surface modification using particle scattering diffusometry. *Biomicrofluidics* **2016**, *10*, 054107. [CrossRef] [PubMed]
42. Grabinski, C.M. *Nanoparticle Deposition and Dosimetry for In Vitro Toxicology*; Case Western Reserve University: Cleveland, HO, USA, 2015.
43. Sousa, V.S.; Teixeira, M.R. Aggregation kinetics and surface charge of CuO nanoparticles: The influence of pH, ionic strength and humic acids. *Environ. Chem.* **2013**, *10*, 313–322. [CrossRef]
44. Martinson, C.A.; Reddy, K. Adsorption of arsenic (III) and arsenic (V) by cupric oxide nanoparticles. *J. Colloid Interface Sci.* **2009**, *336*, 406–411. [CrossRef]
45. Goswami, A.; Raul, P.; Purkait, M. Arsenic adsorption using copper (II) oxide nanoparticles. *Chem. Eng. Res. Des.* **2012**, *90*, 1387–1396. [CrossRef]
46. Cao, A.-m.; Monnell, J.D.; Matranga, C.; Wu, J.-m.; Cao, L.-l.; Gao, D. Hierarchical nanostructured copper oxide and its application in arsenic removal. *J. Phys. Chem. C* **2007**, *111*, 18624–18628. [CrossRef]
47. Kumar, I.; Ranjan, P.; Quaff, A.R. Cost-effective synthesis and characterization of CuO NPs as a nanosize adsorbent for as (III) remediation in synthetic arsenic-contaminated water. *J. Environ. Health Sci. Eng.* **2020**, *18*, 1131–1140. [CrossRef] [PubMed]
48. Singh, D.K.; Verma, D.K.; Singh, Y.; Hasan, S.H. Preparation of CuO nanoparticles using *Tamarindus indica* pulp extract for removal of As (III): Optimization of adsorption process by ANN-GA. *J. Environ. Chem. Eng.* **2017**, *5*, 1302–1318. [CrossRef]